ELSEVIER

Energy and Buildings 33 (2000) 69–73

ENERGY AND BUILDINGS

www.elsevier.com/locate/enbuild

Laminar natural convection in a pitched roof of triangular cross-section: summer day boundary conditions

H. Asan*, L. Namli

Department of Mechanical Engineering, Karadeniz Technical University, 61080 Trabzon, Turkey

Received 15 March 2000; accepted 10 May 2000

Abstract

A numerical study has been carried out for the two-dimensional laminar natural convection in a pitched roof of triangular cross-section under summer day boundary conditions. Stream function-vorticity formulation was applied and control volume integration solution technique is adopted in this study. Solutions are obtained up to Rayleigh number of 10^6. Steady-state solutions have been obtained for height–base ratios of $0.125 \leq L^* \leq 1$. The effects of height–base ratio and Rayleigh number on the flow structure and heat transfer are investigated. It has been found that a considerable proportion of the heat transfer across the base wall of the region takes place near the intersection of the cold horizontal wall and hot inclined wall. The relationship between the mean Nusselt number, Nu_b, the Rayleigh number, Ra, and the height–base ratio, L^*, is such that for equivalent changes in Rayleigh number and height–base ratio, the influence of height–base ratio is the considerable higher factor. Comparisons with earlier works were also made.

Keywords: Natural convection; Roof; Heat transfer

1. Introduction

Natural convection heat transfer and fluid flow in enclosed spaces has been studied extensively in recent years in response to energy-related applications, such as thermal insulation of buildings using air gaps, solar energy collectors, furnaces and fire control in buildings and so on. The enclosures encountered in these applications are highly diverse in their geometrical configuration and the most investigated enclosures include the annulus between horizontal cylinders, the spherical annulus, the closed rectangular cavity and the hollow horizontal cylinder. A great deal of these works dealing with flow and associated heat transfer in enclosures are reported in the cited literature [1–6]. A state of the art review of the most recent literature was given by Fusegi and Hyun [7]. It concentrates on sidewall-heated natural convection flows in rectangular and/or square enclosures. Other enclosures have been investigated to lesser extend [8,9].

This paper pertains to the natural convection flow in an isosceles-triangular enclosure with a horizontal base and heat input through the inclined walls. The work has been motivated by the heat transfer as associated with air-conditioning load calculations for pitched roofs with horizontal suspended ceiling. Also relevant is the heat transfer problem associated with roof-type solar still and various other engineering structures. In spite of its obvious engineering importance, this problem has not been given the attention it deserves and air conditioning calculations involving such configurations have had to be based on published data on pitched roofs with ceilings following the roof contours. The present work aims at obtaining the various heat and flow parameters for such enclosures as described above. Results are presented for the laminar-flow regime only with the added simplifications that the temperature of the heat source (the hypotenuse) is constant.

A schematic diagram of the physical situation is presented in Fig. 1. The inclined (hypotenuse) and base walls are maintained isothermal with $t_H > t_C$, t_H being the inclined wall temperature. These boundary conditions were resembles as summer day boundary conditions where the outside temperature is hot and inside temperature is sustained cold via air conditioning. All the fluid properties are constant except the density variation, which was determined according to the Boussinesq approximation. Stream function-vorticity formulation was applied. A control volume integration solution technique is adopted and convective terms were approxi-

* Corresponding author.

0378-7788/00/$ – see front matter
PII: S0378-7788(00)00066-9

Nomenclature

h	height of the roof (m)
b	half length of horizontal base wall (m)
L^*	height–base ratio, height of roof scaled by half-length of base wall, h/b
t_C	cold wall temperature,(K)
t_H	hot wall temperature (K)
T	dimensionless temperature, $(t-t_C)/(t_H-t_C)$
Pr	Prandtl number
Ra	Rayleigh number
Nu_x	local Nusselt number
Nu_b	mean Nusselt number
Greek symbols	
ω	non-dimensional vorticity
ψ	non-dimensional stream function
Subscripts	
C	cold wall
H	hot wall

mated by upwind differencing scheme and central differencing were used for diffusive terms. Solutions are obtained up to Rayleigh number of 10^6. Six different height–base ratios, L^*, namely 0.125, 0.25, 0.40, 0.60, 0.8 and 1.0 are considered. The effects of height–base ratio and Rayleigh number on the flow structure and heat transfer are investigated.

2. Analysis and numerical method

Fig. 1 shows a schematic diagram of the physical system to be investigated. The roof is filled with a viscous, incompressible Newtonian fluid. The inclined and the base walls are kept at constant temperatures t_H and t_C respectively with $t_H > t_C$ The governing equations for two-dimensional, laminar, incompressible buoyancy-induced flows with Boussinesq approximation and constant fluid properties in non-dimensional stream function vorticity form are:

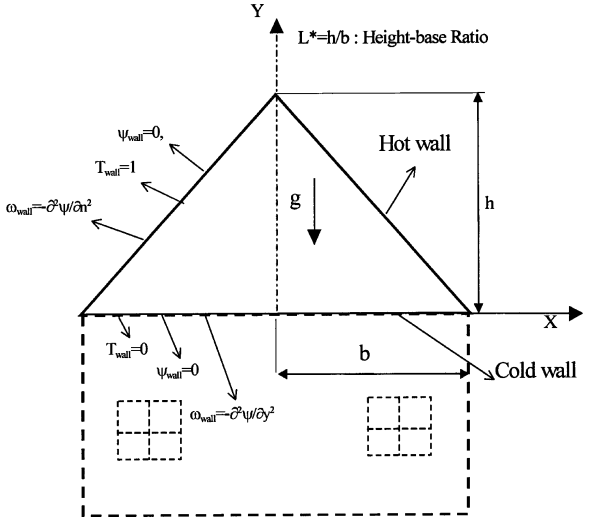

Fig. 1. Geometry of the pitched roof under summer day boundary conditions.

$$\frac{\partial}{\partial x}\left(T\frac{\partial\psi}{\partial y}\right)-\frac{\partial}{\partial y}\left(T\frac{\partial\psi}{\partial x}\right)-\frac{\partial}{\partial x}\left(\frac{1}{Pr}\frac{\partial T}{\partial x}\right)-\frac{\partial}{\partial y}\left(\frac{1}{Pr}\frac{\partial T}{\partial y}\right)=0, \tag{1}$$

$$\frac{\partial}{\partial x}\left(\omega\frac{\partial\psi}{\partial y}\right)-\frac{\partial}{\partial y}\left(\omega\frac{\partial\psi}{\partial x}\right)-\frac{\partial}{\partial x}\left(\frac{\partial\omega}{\partial x}\right)-\frac{\partial}{\partial y}\left(\frac{\partial\omega}{\partial y}\right)=0, \tag{2}$$

$$\frac{\partial^2\psi}{\partial x^2}+\frac{\partial^2\psi}{\partial y^2}=-\omega, \tag{3}$$

where

$$\omega=\frac{\partial v}{\partial x}-\frac{\partial u}{\partial y},\qquad u=\frac{\partial\psi}{\partial y},\qquad v=-\frac{\partial\psi}{\partial x}.$$

Eqs. (1)–(3) are the non-dimensional temperature, vorticity and stream function equations, respectively.

2.1. The non-dimensional boundary conditions

On the horizontal (bottom) wall

$$\psi=0,\qquad \omega_{\text{wall}}=\frac{-\partial^2\psi}{\partial n^2},\qquad T=0.$$

On the inclined walls

$$\psi=0,\qquad \omega_{\text{wall}}=\frac{-\partial^2\psi}{\partial n^2},\qquad T=1,$$

where ω_{wall} is the value of the vorticity at wall and n is the outward drawn normal of the surface. Corner point vorticity values were updated as averages of the two adjacent wall node vorticity values. These boundary conditions were used to update related values on all boundaries of the triangle as the steady-state solutions were numerically approached. The discontinuity in temperature at the intersection of the inclined and base walls was handled by assuming the average temperature of the two walls at the corner and keeping the adjacent nodes with the respective wall temperatures. The inclined boundary (hypotenuse) was approximated staircase-like zigzag lines. Although the solution was computed on the approximated geometry, the resulting error in the solution — for moderately fine grid — is usually surprisingly small.

2.2. Nusselt numbers

The energy transported across the horizontal wall is expressed in terms of local and mean Nusselt numbers. The local Nusselt numbers for the horizontal wall can be

obtained from gradients of temperatures from the following relationship:

$$Nu_x = \left.\frac{\partial T}{\partial y}\right|_{y=0} \tag{4}$$

and mean Nusselt number,

$$\overline{Nu_b} = \frac{1}{b}\int_0^b \left.\frac{\partial T}{\partial y}\right|_{y=0} \mathrm{d}x. \tag{5}$$

The integration of Eq. (5) was performed using the Trapezoidal rule.

The energy transport, vorticity transport and stream function equations together with boundary conditions describe the problem under consideration. In this study, vorticity transport and energy transport equations were solved by employing the alternating direction implicit method (ADI) finite difference technique [10], while the stream function equation was solved by employing the Gaussian successive over-relaxation (SOR) technique [11]. Convective terms were approximated by upwind differencing scheme and central differencing were used for diffusive terms.

To check the validity of the numerical results, test calculations were performed for the following values of the controlling parameters: Pr=0.7, Ra=100. Quantitatively, the program was verified by a comparison with an experimental work performed by El Sherbiny et al. [12], who developed empirical Nusselt number equations for an aspect ratio of 5.0 and a tilt angle of 60°. The results were also verified by comparison with the numerical results of Asan [13]. Grid independent study was performed and a uniform grid system of 51×51 was chosen for the calculation of all cases in this study. Solutions were assumed to converge when the following convergence criteria was satisfied for every variable at every point in the solution domain

$$\left|\frac{\phi_{\mathrm{new}} - \phi_{\mathrm{old}}}{\phi_{\mathrm{new}}}\right| \leq 10^{-4} \tag{6}$$

where ϕ represents ψ, ω and T.

3. Results and discussion

In this study, calculations were carried out for height–base ratios of 0.125, 0.25, 0.40, 0.60, 0.80, 1.0 and Prandtl number of 0.7. Rayleigh numbers were varied from the conduction dominated mode into the laminar free convection region(1×10^3–1×10^6). The influence of Rayleigh number and height–base ratio, L^*, on the flow field and heat transfer is considered first. The average Nusselt numbers are then discussed.

3.1. Flow and isotherm patterns

Fig. 2 represents a series of streamline and isotherm configurations for dimension ratios of 0.25, 0.40, 0.60, 0.80 and 1.0, Prandtl number of 0.7, and Rayleigh numbers of 10^3, 10^4, 10^5 and 10^6. To save space, streamline results are presented on the left half of the triangle and the isotherms are presented in the right half of the triangle. These series of results are designed to show the individual influence of the

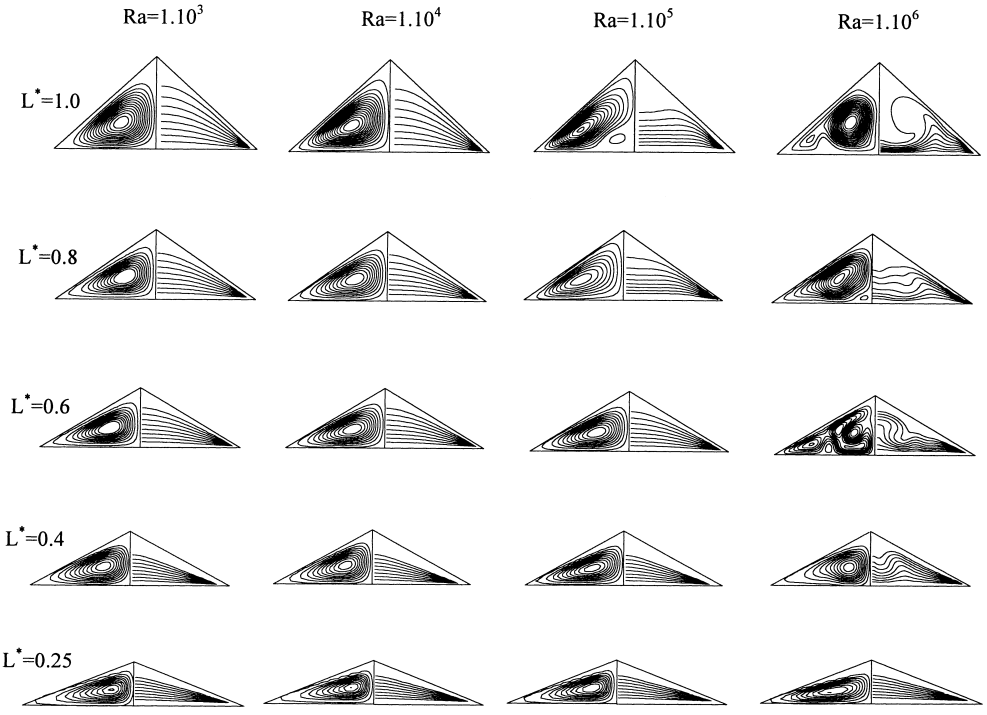

Fig. 2. Streamlines and isotherms for different height–base ratios and Ra numbers.

Rayleigh number and height–base ratio on the flow field and heat transfer.

Since the results for all height–base ratios are similar, only the results for $L^*=1.0$ will be discussed ($L^*=1.0$, $1\times10^3\leq Ra\leq1\times10^6$). The fluid in the bottom portion of the enclosure is relatively stagnant and stays colder. So, the fluid in the close vicinity of the bottom wall has a higher density than that near the inclined hot wall. Thus, the fluid near the surface of the inclined wall moves upward while the relatively heavy fluid near the line of symmetry moves downward. As the fluid moves downward, it loses energy and eventually forces the separation of the thermal boundary layer along the inclined wall. The heavy fluid then enters the thermal boundary layer of the bottom wall and completes the re-circulation pattern. As it seen from Fig. 2, for small Rayleigh numbers, two counter rotating vortices (the right one is not shown) are present in the enclosure and the eye of the vortices is located at center of the half of the cross-section ($Ra=1\times10^3$). As the Rayleigh number is increased, the eye of the vortex slightly moves towards to the inclined wall of the roof ($Ra=1\times10^4$). This increase in Rayleigh number causes more strong cross-sectional flows. Further increase in the Rayleigh number ($Ra=1\times10^5$) causes secondary vortexes to develop on the horizontal wall near to the line of symmetry. The newly developed secondary vortexes pushes the eye of the primary vortexes further towards to the inclined wall as it seen from Fig. 2 ($Ra=1\times10^5$, $L^*=1.0$). Increasing the Rayleigh number beyond 10^5 causes the secondary vortexes to get bigger and primary vortexes to get smaller, as it seen from Fig. 2 ($Ra=1\times10^6$, $L^*=1.0$). The transition from two-vortex solution to multiple vortex solution is Rayleigh number and height–base ratio dependent. As height–base ratio gets smaller, the transition to multiple vortex solution takes place at higher Rayleigh numbers (Fig. 2, $L^*<1.0$, $1\times10^3\leq Ra\leq1\times10^6$).

The results of temperature field are shown in the right half of the triangle in Fig. 2. Here isotherms represent the lines with equal intervals between zero (cold base wall) and unity (hot inclined wall). As it seen from Fig. 2, the isotherms emerge normally from the adiabatic wall (line of symmetry) towards the intersection of the inclined wall and the horizontal bottom wall. For small Rayleigh numbers ($10^4\leq Ra$), the temperature distribution is almost the same as in the pure conduction case. However, for $Ra>10^4$, the natural convection effect is dominant instead of conduction and a temperature inversion appears in the enclosure. As an example, for $Ra=1\times10^5$ and $L^*=1.0$, the effect of the multiple cell solution extends into the region of the enclosure near central region. The isotherms are pushed towards the hot inclined wall for approximately the first quarter of the width of the enclosure near to the corner ($Ra=1\times10^6$, $L^*=1$). On the other hand, the isotherms are pushed downward towards the cold wall near to the line of symmetry. The sudden depression of the near-middle sections of the isotherms indicated the possibility of separation occurring in the primary flow around these sections.

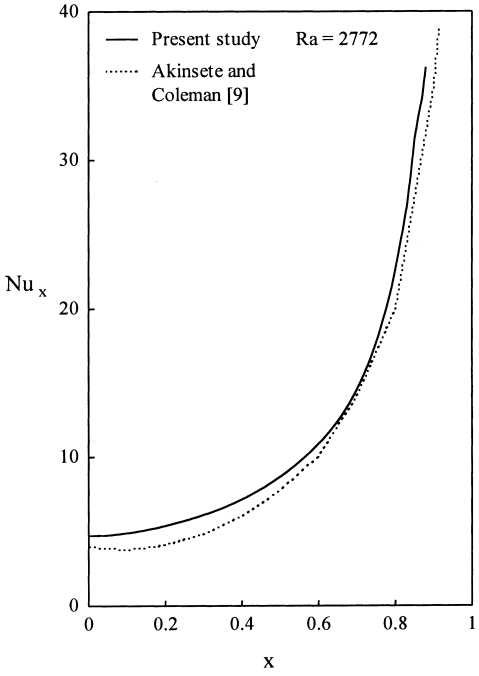

Fig. 3. Local Nusselt number vs. x on the horizontal bottom wall.

3.2. Local and mean Nusselt numbers

As an example, the local Nusselt number variation across the horizontal bottom wall for height–base ratio of 0.25 and Rayleigh number of 2772 is shown in Fig. 3. As it seen from figure, the local Nusselt number increases to definite value at

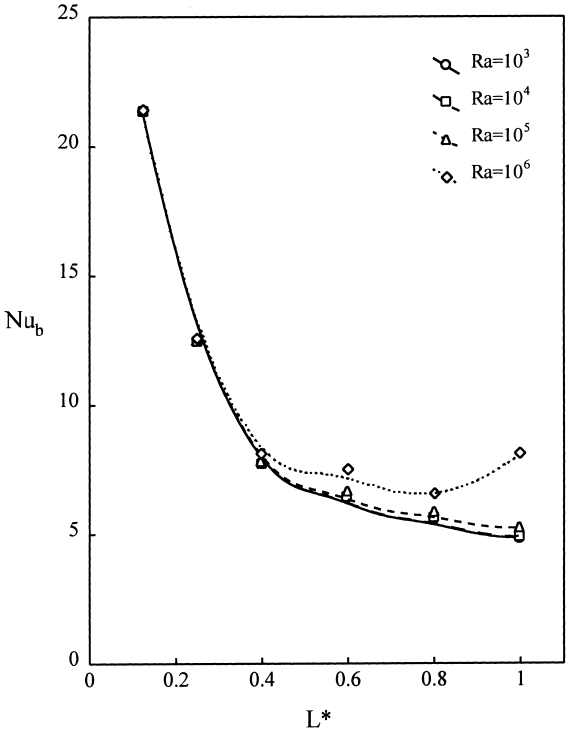

Fig. 4. Mean Nusselt number vs. height–base ratio for different Rayleigh numbers.

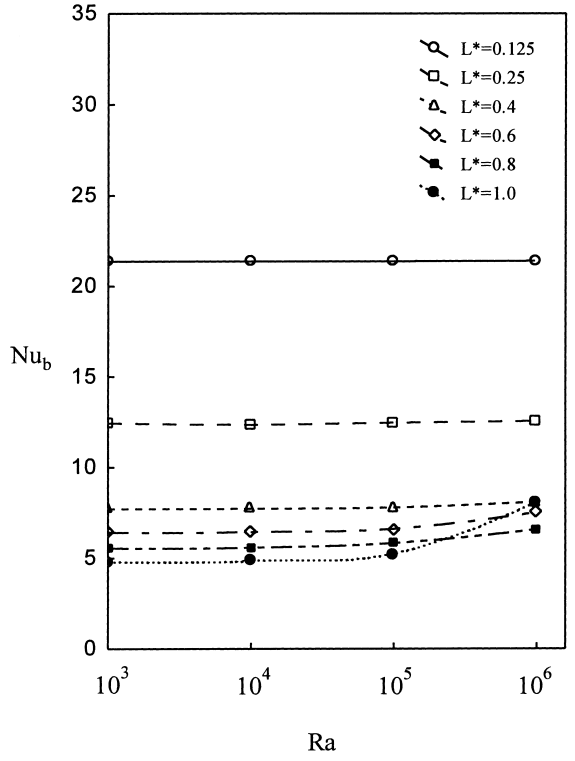

Fig. 5. Mean Nusselt number vs. Rayleigh number for different height–base ratios.

the intersection of cold bottom wall and hot inclined wall. The high values of Nusselt number near the intersection give an indication that a given region within the neighborhood of this intersection accounts for more than a proportionate amount of heat transported across the base wall. Here the comparison with earlier work of Akinsete and Coleman [9] was also made and as it seen the results of present study matches pretty well with earlier results.

The variation of the mean Nusselt number, Nu_b, with height–base ratio, L^*, is shown in Fig. 4. For a given Rayleigh number, increasing the height–base ratio gives rise to sharp drops in the amount of heat transported across the bottom wall of the roof. This results is to be expected because most of the heat transfer across the base wall occurs near the intersection between bottom and inclined walls. So, for a given Rayleigh number, the higher the height–base ratio, the less the heat transfer across the base wall.

The variation of the mean Nusselt number, Nu_b, with Rayleigh number is shown in Fig. 5. As it is seen from figure, Nu_b changes very slightly over most of the ranges of Rayleigh numbers considered. It is noticed that these changes are more pronounced for higher height–base ratios than lower ratios.

4. Conclusions

This paper has reported numerical results for steady, laminar, two-dimensional natural convection in a pitched roof of triangular cross-section under summer day boundary conditions. The results presented show that height–base ratio has a profound influence on the temperature and flow field. On the other hand, the effect of Rayleigh number is not significant for $L^*<1$ and $Ra<10^5$ (Fig. 5). For small Rayleigh numbers, two counter rotating vortices are present in the enclosure and the eye of the vortices is located at center of the half of the cross-section. As the Rayleigh number is increased, the eye of the vortex moves towards to the hot inclined wall. Further increase in the Rayleigh number causes secondary vortexes to develop on the horizontal wall near to the line of symmetry. The newly developed secondary vortexes pushes the eye of the primary vortexes further towards to the inclined wall. The transition from two-vortex solution to multiple vortex solution is Rayleigh number and height–base ratio dependent. As height–base ratio gets smaller, the transition to multiple vortex solution takes place at higher Rayleigh numbers. It has been found that a considerable proportion of the heat transfer across the base wall of the region takes place near the intersection of the cold horizontal wall and hot inclined wall. The relationship between the mean Nusselt number, Nu_b, the Rayleigh number, Ra, and the height–base ratio, L^*, is such that for equivalent changes in Rayleigh number and height–base ratio, the influence of height–base ratio is the considerable higher factor.

References

[1] G.D. Raithby, K.G.T. Hollands, Natural convection, in: W.M. Rohsenow, J.P. Hartnett, E.N. Ganic (Eds.), Handbook of Heat Transfer Fundamentals, 2nd Edition, McGraw-Hill, New York, 1985 (Chapter 6).

[2] K.T. Yang, in: S. Kakac, R.K. Shah, W. Aung (Eds.), Handbook of Single-phase Convective Heat Transfer, Wiley/Interscience, New York, 1987 (Chapter 13).

[3] S. Ostrach, Natural convection in enclosures, J. Heat Transfer 110 (1988) 1175–1190.

[4] I. Goldhirsch, R.B. Pelz, S.A. Orszag, Numerical simulation of thermal convection in a two-dimensional finite box, J. Fluid Mech. 199 (1989) 1–28.

[5] E.E. Selamet, V.S. Arpaci, C. Borgnakke, Simulation of laminar buoyancy-driven flows in an enclosure, Numer. Heat Transfer, Part A 22 (1992) 401–420.

[6] M.R. Ravi, R.A.W. Henkes, C.J. Hoogendoorn, On the high-Rayleigh number structure of steady laminar natural-convection flow in a square enclosure, J. Fluid Mech. 262 (1994) 325–351.

[7] T. Fusegi, J.M. Hyun, Laminar and transitional natural convection in an enclosure with complex and realistic conditions, Int. J. Heat Fluid Flow 15 (4) (1994) 258–267.

[8] J.H. Lee, T.S. Lee, Natural convection in the annuli between horizontal confocal elliptic cylinders, Int. J. Heat Mass Transfer 24 (1981) 1739.

[9] V.A. Akinsete, T.A. Coleman, Heat transfer by steady laminar free convection in triangular enclosures, Int. J. Heat Mass Transfer 25 (1982) 991.

[10] P.J. Roache, Computational Fluid Dynamics, Hermosa, Albuquerque, NM, 1982.

[11] D. Young, Iterative methods for solving partial differential equations of elliptical type, Trans. Am. Math. Soc. 76 (1954) 92.

[12] S.M. El Sherbiny, G.D. Raithby, K.G.T. Hollands, Heat transfer by natural convection across vertical and inclined air layers, J. Heat Transfer 96 (1982) 104.

[13] H. Asan, Natural convection in an annulus between two isothermal concentric square ducts, Int. Com. Heat Mass Transfer, 2000, in press.